Synthesis and Reactivity of Novel Alkali Metal Stannides

Thorsten Schollmeier[b], Ulrich Englich[c], Roland Fischer[a], Ingo Prass[b], Karin Ruhlandt[c], Markus Schürmann[b], and Frank Uhlig[a]

[a] Institut für Anorganische Chemie, Technische Universität Graz, Stremayrgasse 16, A-8010 Graz, Austria
[b] Fachbereich Chemie der Universität Dortmund, Anorganische Chemie II, Otto-Hahn-Straße 6, D-44221 Dortmund, Germany
[c] Syracuse University, Department of Chemistry, 1-014 Center of Science and Technology, Syracuse, N.Y., USA

Reprint requests to Prof. Dr. F. Uhlig. Fax: +43-316-873-8701. E-mail: frank.uhlig@tugraz.at

Z. Naturforsch. **59b,** 1462 – 1470 (2004); received August 24, 2004

Dedicated to Professor Hubert Schmidbaur on the occasion of his 70th birthday

Reactivity and side products of reactions of diorganodihydridostannanes (R_2SnH_2, R = Me, ^{n}Bu, ^{t}Bu)) with various alkali metal compounds have been discussed. Alternatively, the synthesis and characterization of a family of novel potassium stannides are described as well. The compounds of type (RR'$_2$Si)R"$_2$SnK (R, R'= Me, Ph; R"= , Me, ^{t}Bu, Ph) **4 – 9** were synthesized by reaction of potassium hydride with bis(silyl)stannides ((RR'$_2$Si)$_2$SnR"$_2$). All compounds were characterized by multinuclear NMR spectroscopy. In addition, the tri-*tert*-butyltin compound **3** (LiSn^{t}Bu$_3$) and the unsymmetrical silyl substituted stannane **10** were characterized by X-ray crystallography.

Key words: Alkali Metal Stannides, Preparation, Reactivity, ^{119}Sn and ^{29}Si NMR Spectroscopy, Structure Elucidation

Introduction

A number of triorgano substituted alkali metal stannides (**A**) is known from literature and has found widespread use in different types of organic and organometallic reactions [1]. However, compounds of type M-SnR$_2$Z (**B**), where is Z at least one "reactive" group such as for example hydrogen, halogen or a triorganosilyl moiety are still rather exotic species and only very few examples have been reported [2 – 6].

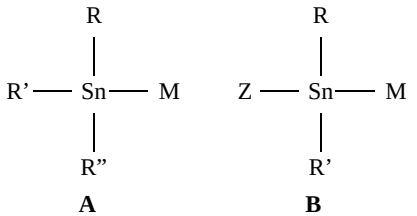

R, R', R" = alkyl, aryl
Z = H, halogene, R_3Si
M = Li, Na, K, Rb, Cs

Scheme 1. Functionalized and non-functionalized organostannides.

Nevertheless such reactive groups Z are necessary for the build up of more complex structures. For example we described recently the exploration of synthetic avenues, structural features, and the reactivity of linear (^{t}Bu$_2$Sn(Z)-(SiMe$_2$)$_n$-Sn(Z)^{t}Bu$_2$; Z = H, Cl, Br, Me$_3$Si, Li; $n = 1 - 6$) [7 – 11] and branched (MeSi[SiMe$_2$-Sn(Z)R$_2$]$_3$; Z = H, Me, Ph, Cl, Br, R = Me, ^{t}Bu, Ph) [12] stannaoligosilanes (eq. (1 – 4)).

$$\mathrm{LiR} + {}^t\mathrm{Bu_2SnH_2} \longrightarrow {}^t\mathrm{Bu_2Sn(H)Li} + \mathrm{RH} \quad (1)$$

$$2\,{}^t\mathrm{Bu_2Sn(H)Li} + \mathrm{Cl\text{-}(SiMe_2)_{\mathit{n}}\text{-}Cl} \longrightarrow \mathrm{H}{}^t\mathrm{Bu_2Sn\text{-}(SiMe_2)_{\mathit{n}}\text{-}Sn}{}^t\mathrm{Bu_2H} + 2\,\mathrm{LiCl},\ n = 1\text{-}6 \quad (2)$$

$$3\,{}^t\mathrm{Bu_2Sn(H)Li} + \mathrm{MeSi[(SiMe_2)\text{-}Cl]_3} \longrightarrow \mathrm{MeSi(SiMe_2Sn}{}^t\mathrm{Bu_2H)_3} + 3\,\mathrm{LiCl} \quad (3)$$

$$\mathrm{RSiMe_2Sn}{}^t\mathrm{Bu_2H} \xrightarrow{\mathrm{CCl_4,\,CHBr_3}} \mathrm{RSiMe_2Sn}{}^t\mathrm{Bu_2X},\ \mathrm{X = Cl, Br} \quad (4)$$

Such chain type stannasilanes containing functional groups are potential precursors for the synthesis of polymeric materials as well as the formation of cyclic or dendrimeric derivatives. Our special interest is focused on cyclic silicon and tin containing

0932–0776 / 04 / 1100–1462 $ 06.00

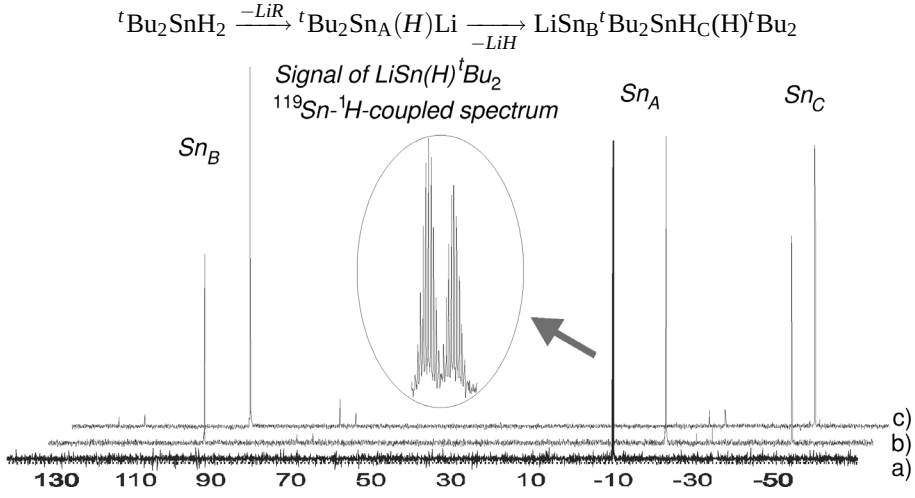

Fig. 1. Time dependent ^{119}Sn NMR spectroscopy proofing the formation of **2**. a) After a period of 4 h; b) after a period of 72 h; c) after 5 – 7 d (identical with a comparable spectra resulting from the reaction of $^{t}Bu_2Sn(H)$-$Sn(H)^{t}Bu_2$ with lithium diisopropylamide (LDA) [13]).

compounds due to their possible applications in ring opening polymerizations as well as their differences in structural and spectroscopic features in comparison to well known cyclic oligosilanes.

Key step of these syntheses is the formation of lithium di-*tert*-butylstannide ($LiSn(H)^{t}Bu_2$ (**1**) see eq. (1)). Unfortunately, this reaction pathway brings along a large number of disadvantages. Unexpected side reactions are usual and the outcome of the reaction depends on the conditions in a complicated and hardly predictable way (*i.e.* solvent system, concentration, metallating agent, reaction time a. s. o.).

This paper is one attempt to explain some of these side reactions, and how to avoid them by carefully choosing the reaction conditions or by using silyl substituted stannanes $(Me_3Si)_2SnR_2$ as starting materials instead of the dihydrido derivatives R_2SnH_2.

Results and Discussion

Although stannyl mono- and dihydrides can conveniently be prepared reports on metallation reactions of these compounds are scarce. Due to the difficulties when trying to metallate hydrostannanes it is not surprising that only a small number of reactions have been reported in literature and no generally applicable method has been suggested so far. A brief summary about methods proposed in literature is given in Table 1.

In 1996 Jousseaume and coworkers [4] published a remarkable and elegant synthesis towards lithiumdiorganostannides by reacting lithiumdiisopropylamide with diorganodihydridostannanes (see eq. (1)).

Table 1. Metallation of hydridostannanes reported in literature.

Starting material	Metallating reagent	Product	Solvent	Ref.
Ph_3SnH	MeLi	Ph_3SnLi	Et_2O, THF	[4, 14]
$^{n}Bu_3SnH$	LDA	$^{n}Bu_3SnLi$	THF	[15]
R_3SnH (R = Ph, Bu)	KH, NaH	R_3SnM	Et_2O, THF, DME	[16]
$^{n}Bu_3SnH$	^{n}BuLi	$^{n}Bu_3SnLi$	THF	[17]
Ph_3SnH	^{n}BuLi	Ph_3SnLi	PMDETA, toluene	[18]
$RR'SnH_2$ (R = Tb, Tip, Mes)	^{t}BuLi	RR'SnHLi	THF	[3]
R_2SnH_2 (R=^{n}Bu, cy)	LDA	R_2SnHLi	THF	[4, 14]

Our investigations using di-*tert*-butylstannane as starting material revealed that the corresponding reactions with ^{t}BuLi or $MN(SiMe_3)_2$ (M = Na, K) are surprisingly time dependent. The reaction with ^{t}BuLi according to eq. (1) is quantitative after 30 min., however, after a period of 12 – 48 h a significant amount of the $LiSn(H)^{t}Bu_2$ (**1**) is converted into the monolithiated distannane **2** ($LiSn^{t}Bu_2$-$Sn(H)^{t}Bu_2$). The formation of compound **2** is quantitative at least after a period of 5 – 7 days. A series of ^{119}Sn NMR spectra proofing this fact is shown in Fig. 1.

A higher concentration of $LiSn(H)^{t}Bu_2$ (**1**) leads to a faster conversion into the monolithiated distannane **2** (Scheme 2) as one would expect for dimerization processes. The byproduct lithiumhydride was isolated and proven by titration with HCl. Similar results are observed for the use of *tert*-butyl lithium instead

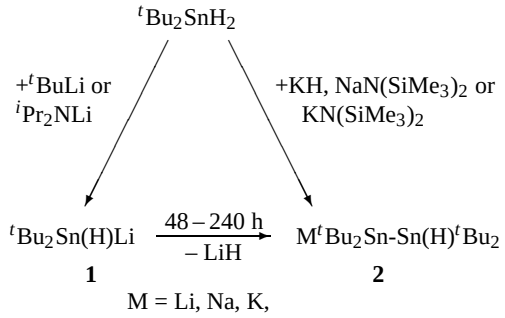

Scheme 2. Chemical reactivity of ^{t}Bu$_2$SnH$_2$ with alkali metal derivatives.

of LDA as metallating reagent. A comparable coupling reaction yielding $Me_3SnSnMe_3$ and LiH starting from Me_3SnH and LDA was previously described by Kuivila and coworkers [19].

We tried to avoid this unexpected coupling reaction by using other alkali metal derivatives, however it could clearly be shown that the conversion of the ^{t}Bu$_2$SnH$_2$ into the monometallated distannane **2** is much faster when using alkali metal bis(trimethylsilyl)amides (MN(SiMe$_3$)$_2$, M = Na, K) or potassium hydride. In both cases only the formation of the monometallated distannane **2** is observed. No evidence for the formation of a MSn(H)^{t}Bu$_2$ species was found suggesting that formation of compound **2** is the rate determining step. This fact may be due to the higher nucleophilicity of sodium or potassium stannides in comparison to the lithium derivatives. We reported the formation of derivative **2**, its reactivity and the NMR spectroscopic details in the reaction of ^{t}Bu$_2$Sn(H)-Sn(H)^{t}Bu$_2$ with various alkali metal derivatives recently [13].

The situation becomes a lot more complex when other diorganodihydridostannanes (R$_2$SnH$_2$, R = alkyl) are investigated. We like to underline this fact by one example only. In contrast to di^{t}butylstannane the reactions of sterically less hindered dialkylstannanes with *tert*-butyl lithium do not yield the expected lithiumstannides. Instead a complex mixture of different tetraorgano tin compounds is obtained as reactions of the alkyl groups including migration, metallation and insertion come into play (Scheme 3).

Formation of the finally obtained reaction products obviously proceeds *via* a series of intermediates. Again, similar reactions were investigated by Kuivila in 1985 for methyltin derivatives [21] and a detailed discussion would go beyond the topic of this paper. Nevertheless the possibility of an organyl group migration from lithium to a Sn-H function was reported for the first time by Wittig, Meyer and Lange in 1951 [14]. The difference in reactivity may be understood in terms of the different nucleophilicity and basicity of methyl and phenyl lithium (Scheme 4).

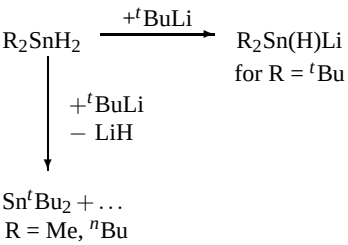

Scheme 3. Reactivity of different diorganostannanes with ^{t}BuLi.

Scheme 4. Substitution versus metallation of Ph_3SnH with different RLi.

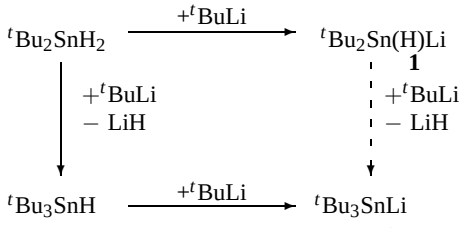

Scheme 5. Formation of ^{t}Bu$_3$SnLi (**3**) from ^{t}Bu$_2$SnH$_2$.

We observed such migration reactions also for the di^{t}butylstannane (^{t}Bu$_2$SnH$_2$) but in this case they are only side reactions with minor importance (Scheme 4) with a yield of less than 5% whereas ^{t}Bu$_2$Sn(H)Li (**1**) is the major product. ^{t}Bu$_3$SnLi (**3**) is most probably formed *via* a ^{t}Bu$_3$SnH intermediate as substitution reactions on ^{t}Bu$_2$Sn(H)Li with excess ^{t}BuLi never proved to happen (Scheme 5).

We were able to isolate derivative **3** by fractionated crystallisation and to confirm the structure by X-ray analysis. Fig. 2 displays the solid state structure of compound **3**, consisting of a cation and an anion with a direct lithium-tin contact.

The lithium atom is surrounded by one ^{t}Bu$_3$Sn unit, in addition to three thf molecules, resulting in an overall coordination number of four. The coordination sphere exhibits a slight distortion from ideal tetrahedral geometry. The Li-O distances range from 1.91(2) to 1.956(9) Å, while the Li-Sn distance is observed at 2.876(14) Å. This is in the range of a direct tin-lithium contact (sum of covalent radii = 2.75 Å). The value is

Table 2. Crystal data and structure refinement for **3** and **10**.

	3	**10**
Formula	$C_{24}H_{51}LiO_3Sn$	$C_{29}H_{42}Si_2Sn$
fw [g/mol]	513.28	565.60
Crystal system	orthorhombic	monoclinic
Crystal size [mm^3]	0.10×0.80×0.80	0.40×0.40×0.30
Space group	*Pbcm*	$P2_1/c$
a [Å]	9.4020(1)	11.405(1)
b [Å]	15.4299(2)	29.882(2)
c [Å]	19.5664(3)	17.079(1)
β [°]	90	90.741(1)
V [Å^3]	2838.54(6)	5826.5(5)
Z	4	8
ρ_{calcd} [g/cm^3]	1.201	1.289
μ [mm^{-1}]	0.918	0.973
$F(000)$	1088	2352
θ Range [°]	3.00 to 27.48	1.37 to 28.31
Index ranges	$-12 \le h \le 12$	$-13 \le h \le 14$
	$-24 \le k \le 24$	$-36 \le k \le 39$
	$-20 \le l \le 20$	$-22 \le l \le 12$
No. of reflections collected	17773	39450
No. of indep reflns/R_{int}	3275 / 0.032	14130 / 0.1283
GooF (F^2)	1.201	0.870
$R1(F)(I > \sigma 2(I))$	0.0492	0.0556
$wR2(F^2)$ (all data)	0.1349	0.0967
Largest diff. peak/hole [e/Å^3]	0.711 / −0.730	0.765 / −1.206

$R1 = \Sigma||F_o| - |F_c||/\Sigma|F_o|$, $wR2 = \sqrt{\Sigma w\{(F_o)^2 - (F_c)^2\}/\Sigma w\{(F_o)^2\}^2}$.

Table 3. Selected bond lengths (Å) for compounds **3**.

Sn(1)-C(5)	2.259(14)	C(5)-C(7)	1.49(2)
Sn(1)-C(9)	2.261(12)	C(5)-C(8)	1.546(17)
Sn(1)-C(1)	2.265(12)	C(5)-C(6)	1.547(19)
Sn(1)-Li(1)	2.876(14)	C(9)-C(12)	1.522(16)
O(1)-C(25)	1.327(14)	C(9)-C(10)	1.535(18)
O(1)-C(28)	1.458(15)	C(9)-C(11)	1.555(18)
O(1)-Li(1)	1.956(9)	C(21)-C(22)	1.494(16)
O(2)-C(21)	1.261(13)	C(22)-C(23)	1.629(14)
O(2)-C(24)	1.673(13)	C(23)-C(24)	1.516(17)
O(2)-Li(1)	1.910(15)	C(25)-C(26)	1.52(3)
C(1)-C(2)	1.521(17)	C(26)-C(27)	1.54(3)
C(1)-C(3)	1.532(15)	C(27)-C(28)	1.50(2)
C(1)-C(4)	1.557(16)		

also comparable with the Sn-Li distance of 2.87 Å in Li(PMDTA)$SnPh_3$ [21] one of only three examples for alkali metal triorganostannides with a direct tin-alkali metal contact ([K(η^6-C_6H_5Me)$_3$Sn(CH_2-^{t}Bu)$_3$] [22]).

The [Sn^{t}Bu$_3$]$^-$ anion exhibits also a distortion from tetrahedral geometry. The average of the C-Sn-C angles is around 103°. This angle is slightly larger than the angles observed for [K(η^6-C_6H_5Me)$_3$Sn(CH_2-^{t}Bu)$_3$] (average C-Sn-C angles of 91.7° [22]), and Li(PMDTA)$SnPh_3$ (PMDTA = ($Me_2NCH_2CH_2$)$_2$NMe) (average C-Sn-C angles of 96.1° [21]) but can be simply explained by the sterically more demanding ^{t}butyl groups. This significant

Table 4. Selected bond angles (°) for compounds **3**.

C(5)-Sn(1)-C(9)	104.1(5)	C(3)-C(1)-Sn(1)	105.4(7)
C(5)-Sn(1)-C(1)	102.0(5)	C(4)-C(1)-Sn(1)	107.4(8)
C(9)-Sn(1)-C(1)	102.8(4)	C(7)-C(5)-C(8)	106.1(11)
C(5)-Sn(1)-Li(1)	114.0(4)	C(7)-C(5)-C(6)	108.0(14)
C(9)-Sn(1)-Li(1)	115.9(3)	C(8)-C(5)-C(6)	107.2(11)
C(1)-Sn(1)-Li(1)	116.1(4)	C(7)-C(5)-Sn(1)	110.6(10)
C(25)-O(1)-C(28)	110.5(9)	C(8)-C(5)-Sn(1)	116.8(9)
C(25)-O(1)-Li(1)	131.9(9)	C(6)-C(5)-Sn(1)	107.8(8)
C(28)-O(1)-Li(1)	115.3(7)	C(12)-C(9)-C(10)	109.0(11)
C(21)-O(2)-C(24)	102.9(9)	C(12)-C(9)-C(11)	107.2(11)
C(21)-O(2)-Li(1)	145.5(8)	C(10)-C(9)-C(11)	109.0(12)
C(24)-O(2)-Li(1)	111.5(5)	C(12)-C(9)-Sn(1)	117.0(8)
O(2)-Li(1)-O(1a)1	102.9(5)	C(10)-C(9)-Sn(1)	107.8(10)
O(2)-Li(1)-O(1)	102.9(5)	C(11)-C(9)-Sn(1)	106.6(7)
O(1a)1-Li(1)-O(1)	102.9(7)	O(2)-C(21)-C(22)	119.2(11)
O(2)-Li(1)-Sn(1)	112.7(6)	C(21)-C(22)-C(23)	102.7(9)
O(1a)1-Li(1)-Sn(1)	116.8(4)	C(24)-C(23)-C(22)	102.0(10)
O(1)-Li(1)-Sn(1)	116.8(4)	C(23)-C(24)-O(2)	104.2(10)
C(2)-C(1)-C(3)	108.4(11)	O(1)-C(25)-C(26)	108.9(16)
C(2)-C(1)-C(4)	108.0(10)	C(25)-C(26)-C(27)	101(2)
C(3)-C(1)-C(4)	108.8(9)	C(28)-C(27)-C(26)	106.2(15)
C(2)-C(1)-Sn(1)	118.5(8)	O(1)-C(28)-C(27)	105.3(11)

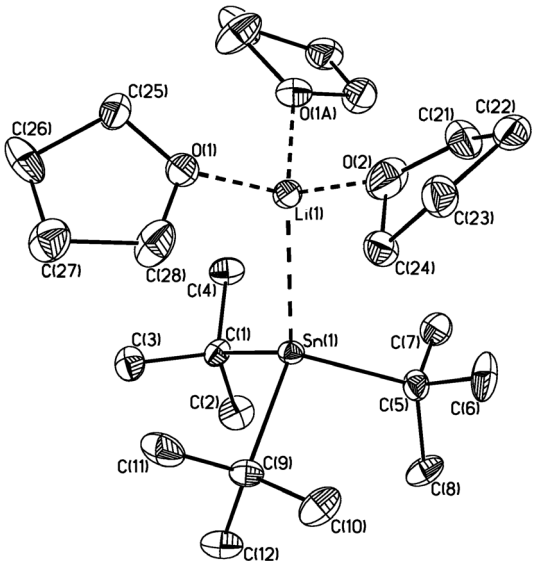

Fig. 2. General view (SHELXTL) of the molecule **3** showing 30% probability displacement ellipsoids and the atom numbering scheme. (Symmetry transformations used to generate equivalent atoms: $a = x, y, 0.5 - z$).

pyramidal geometry in such triorganotin units has been explained by a high *p*-character in the tin-carbon bond, affected by the differences in energy between the *s* and *p* orbitals [21–23]. Consequently, the lone pair, and the tin-alkali metal bond possess high *s*-character explaining the similar geometries between the separated and contact species of triorganostannides [23].

			$(RR'_2Si)_2SnR''_2$				$(RR'_2Si)_2R''_2SnK$		
R	R'	R"	$\delta_{^{29}Si}$	$\delta_{^{119}Sn}$	$^1J_{^{29}Si-^{119/117}Sn}$		$\delta_{^{29}Si}$	$\delta_{^{119}Sn}$	$^1J_{^{29}Si-^{119/117}Sn}$
			[ppm]		[Hz]		[ppm]		[Hz]
Me	Me	Me	−10.4	−274.4	525/501	**4**	−8.4	−346.8	456/436
Me	Me	Ph	−7.0	−255.2	520/497	**5**	−9.7	−227.0	402/384
Ph	Me	Me	−12.8	−269.9	525/500	**6**	−14.7	−349.4	401/383
Me	Ph	^{t}Bu	−10.3	−188.2	385/368	**7**	−9.3	5.2	[a,b]
Ph	Ph	Me	−8.72	−264.9	536/512	**8**	−9.0	−330	[a]
Ph	Ph	^{t}Bu	−7.46	−170.6	348/333	**9**	−6.9	−4.8	663/634

Table 5. ^{119}Sn and ^{29}Si NMR data of $(RR'_2Si)_2SnR''_2$ and the resulting stannides **4**–**9** (solvent C_6D_6).

[a] No coupling observed, broad lines, half width > 250 Hz; [b] solvent: D_2O-cap./*n*-hexane.

Selected bond lengths, angles and further crystallographic details are given in Tables 2–4.

As conclusion it should be marked that all metallation reactions with dihydridotin derivatives must be carried out under strictly controlled reaction conditions and on a defined time scale to omit the formation of unwanted side products.

Problems with migration of hydrido-groups or self condensation reactions of metallated stannanes under formation of a complex product mixture can easily be overcome when triorganosilyl groups as masked hydrido functionalities are used. Cleavage of Si-Sn bonds by various metallating agents has intensely been studied in the past and was recently reviewed [1]. However, to the best of our knowledge no successful attempts to cleave silicon-tin bonds with potassium hydride to give potassium stannides have been reported so far. Reaction of bis(triorganosilyl)diorganostannanes ($(RR'_2Si)_2SnR''_2$, R, R', R"= alkyl, aryl) with potassium hydride in the presence of crown ether (18crown6) in dimethoxyethane (DME) was found to be a fast and convenient method for the preparation of the corresponding stannide derivatives of potassium (eq. (5)).

$$(RR'_2Si)_2SnR''_2 \xrightarrow[-RR'_2SiH]{+KH} \underset{(\mathbf{4}-\mathbf{9})}{(RR'_2Si)R''_2Sn-K} \quad (5)$$

Comp.	R	R'	R"	RR'_2SiH
4	Me	Me	Me	Me_3SiH
5	Me	Me	Ph	Me_3SiH
6	Ph	Me	Me	$PhMe_2SiH$
7	Me	Ph	^{t}Bu	Ph_2MeSiH
8	Ph	Ph	Me	Ph_3SiH
9	Ph	Ph	^{t}Bu	Ph_3SiH

The ^{119}Sn and ^{29}Si NMR data of the starting materials as well as of the resulting stannides **4**–**9** are summerized in Table 5. Tetrahydrofuran (thf) can be used instead of the DME, however, one has to expect side reactions as well as longer reaction times. Triorganosilanes of type RR'_2SiH are formed as second reaction products and were identified *via* ^{29}Si NMR spectroscopy (Me_3SiH, $\delta_{^{29}Si}$: −16.5 ppm; $PhMe_2SiH$, $\delta_{^{29}Si}$: −17.3 ppm; $MePh_2SiH$, $\delta_{^{29}Si}$: −17.6 ppm; Ph_3SiH, $\delta_{^{29}Si}$: −18.2 ppm). With the exception of the triphenylsilane these hydridosilanes can be separated from the reaction mixture by condensation in vacuum very easily.

The resulting stannides **4**–**9** are now useful starting materials for a huge number of reactions not only in Si-Sn chemistry, especially due to the remaining highly reactive triorganosilyl group in the molecule. For example, the stannides **7** and **9** can be converted easily into unsymmetrical disilylstannanes **10** and **11** (eq. (6)). The yields are nearly quantitative and we were able to isolate both compounds as colourless crystals.

$$\underset{\mathbf{7}\ \mathbf{9}}{(RR'_2Si)^tBu_2Sn\text{-}K} \xrightarrow[-KCl]{+PhMe_2SiCl} \underset{\mathbf{10}\ \mathbf{11}}{RR'_2Si\text{-}^tBu_2Sn\text{-}SiPhMe_2} \quad (6)$$

R = Me; R'=Ph

R = R' = Ph

The first synthesis of derivative **10** on another reaction pathway was described recently, this time we were able to isolate good quality crystals useful for X-ray analysis. These crystals were obtained by crystallization from *n*-hexane. Derivative **10**, depicted in Fig. 3, exhibits an almost perfect tetrahedral geometry around the silicon and tin atoms. Small deviations from tetrahedral geometry are due to the sterically more demanding *tert*-butyl groups at the tin atom.

The Sn-Si bond lengths are 2.599(1) for the Sn(1)-Si(1) and 2.602(2) for the Sn(1)-Si(2). Sn-C contacts are observed between 2.191(5) (Sn(1)-C(34)) and 2.209(5) (Sn(1)-C(30)). The Si-phenyl distances are around 1.875 and the Si-methyl distances differ between 1.689(5) and 1.691(5). All of these values are in a good accordance with those of compounds reported recently [7, 8]. Additional crystallographic details are

Table 6. Selected bond lengths (Å) for compounds **10**.

Sn(1)-Si(1)	2.602(2)	Si(1)-C(9)	1.875(6)
Sn(1)-Si(2)	2.599(1)	Si(1)-C(15)	1.875(5)
Sn(1)-C(1)	2.191(5)	Si(2)-C(17)	1.875(5)
Sn(1)-C(5)	2.209(5)	Si(2)-C(29)	1.869(5)

Table 7. Selected bond angles (°) for compounds **10**.

Si(1)-Sn(1)-Si(2)	108.02(5)	C(9)-Si(1)-C(15)	106.9(3)
C(1)-Sn(1)-C(5)	111.2(2)	C(9)-Si(1)-C(16)	107.8(2)
C(1)-Sn(1)-Si(1)	111.5(1)	C(15)-Si(1)-C(16)	110.5(2)
C(1)-Sn(1)-Si(2)	112.0(1)	C(17)-Si(2)-Sn(1)	113.3(2)
C(5)-Sn(1)-Si(1)	107.3(1)	C(23)-Si(2)-Sn(1)	110.2(2)
C(5)-Sn(1)-Si(2)	106.7(1)	C(29)-Si(2)-Sn(1)	107.8(2)
C(9)-Si(1)-Sn(1)	111.1(2)	C(17)-Si(2)-C(23)	109.9(2)
C(15)-Si(1)-Sn(1)	112.5(2)	C(17)-Si(2)-C(29)	106.6(2)
C(16)-Si(1)-Sn(1)	108.0(2)	C(23)-Si(2)-C(29)	108.9(2)

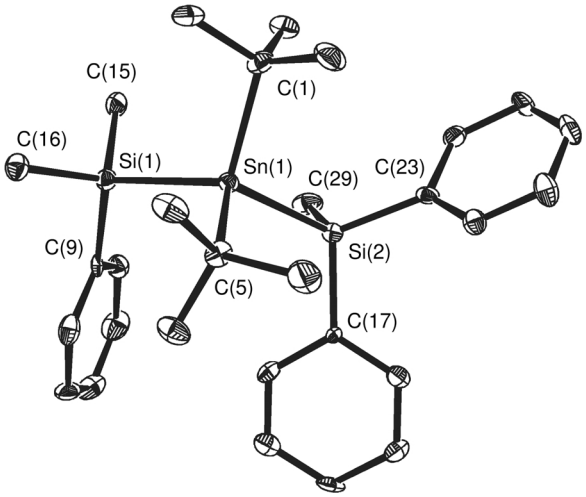

Fig. 3. General view (SHELXTL) of the molecule **10** showing 50% probability displacement ellipsoids and the atom numbering scheme.

given in Tables 2, 6 and 7, the experimental section, as well as in the supplementary material.

One of the main goals of our chemistry is still the synthesis of precursors for Si-Sn materials; nevertheless, this contribution is a side product of this chemistry potentially useful also for chemists beyond the circle of Si-Sn specialists. A more detailed study on cleavage reactions of silicon tin bonds with various other metallating reagents will be reported shortly [24].

Experimental Section

General methods

All reactions were carried out under an atmosphere of inert gas (N_2 or Ar) using Schlenk techniques. All solvents were dried by standard methods and freshly distilled prior to use. The bis(silyl)stannanes used as starting materials were prepared according to published procedures [7, 8, 25]. All other chemicals used as starting materials were obtained commercially. ^{1}H and ^{13}C NMR spectra were recorded using a Bruker DPX 400 spectrometer. ^{29}Si and ^{119}Sn NMR spectra were measured using a Bruker DPX 400, a Bruker DRX 300, or a Varian Inova 300 MHz spectrometer. Internal standards were Me_4Si and Me_4Sn. If not stated otherwise, the NMR experiments were carried out ^{1}H decoupled. GC-MS analyses were recorded using a Finnigan ETD 800. Elemental analyses were performed on a LECO-CHNS-932 analyzer.

Selected reactions of R_2SnH_2 with alkali metal reagents, MR

General procedure

6.4 mmol of an alkali metal reagent (^{t}BuLi, $(Me_3Si)_2NM$, LDA, KH) and 15 ml thf were placed in a 50 ml Schlenk vessel. The solution was cooled down and 6.4 mmol of the diorganodihydridostannane were added *via* a syringe. The solution was stirred x h at the given temperatures and additional 12 h at room temperature. The resulting mixtures were examined by ^{119}Sn NMR spectroscopy.

Reactions with ^{t}Bu$_2$SnH$_2$,
starting material: 1.5 g (6.4 mmol) ^{t}Bu$_2$SnH$_2$

a) With ^{t}BuLi at 0 °C

$x = 2$ h; – ^{119}Sn{^{1}H} NMR (111.92 MHz, D_2O-capillary): **1** [10%]: $\delta = -9.8$ (s, $^1J(^{119}\text{Sn-}^1\text{H})$=287 Hz); ^{t}Bu$_2$Sn(H)-Sn(H)^{t}Bu$_2$ [40%]: $\delta = -83.4$ (s); ^{t}Bu$_2$SnH$_2$ [10%]: $\delta = -117.0$ (s); not classified signals: [10%] $\delta = -18.5$; [5%] $\delta = -22.9$; [20%] $\delta = -34.4$; [5%] $\delta = -49.4$.

b) With ^{t}BuLi at −45 °C

$x = 4$ h; – ^{119}Sn{^{1}H} NMR (111.92 MHz, D_2O-capillary): **1** [100%]: $\delta = -9.7$ (s, $^1J(^{119}\text{Sn-}^1\text{H})$=287 Hz). Evaporation of the solvent and crystallisation attempts with *n*-hexane gave ∼ 50 mg of colourless crystals of compound **3**.

$x = 72$ h; – ^{119}Sn{^{1}H} NMR (111.92 MHz, D_2O-capillary): **1** [50%]: $\delta = -5.8$ (s, $^1J(^{119}\text{Sn-}^1\text{H})$=287 Hz); ^{t}Bu$_2Sn_A$(H)Sn$_B^{t}Bu_2$Li, **2** [50%]: $\delta = 137.7$; −42.6 ($^1J(^{119}\text{Sn-}^{119/117}\text{Sn})$=6930/6610 Hz).

$x = 120$ h at −45 °C, 48 h at r.t.; – ^{119}Sn{^{1}H} NMR (111.92 MHz, D_2O-capillary): ^{t}Bu$_2$Sn$_A$(H)Sn$_B$^{t}Bu$_2$Li, **2** [> 90%]: $\delta = 134,4$; −43.2 ($^1J(^{119}\text{Sn-}^{119/117}\text{Sn})$=6930/6610 Hz).

c) With LDA at −50 °C

$x = 4$ h; – ^{119}Sn{^{1}H} NMR (111.92 MHz, D_2O-capillary): **1** [100%]: $\delta = -9.7$ (s, $^1J(^{119}\text{Sn-}^1\text{H}) = 287$ Hz).

$x = 72$ h; – ^{119}Sn{^{1}H} NMR (111.92 MHz, D_2O-capillary): **1** [45%]: $\delta = -6.0$ (s, $^1J(^{119}\text{Sn-}^1\text{H}) = 286$ Hz); $^t\text{Bu}_2\text{Sn}_\text{A}(\text{H})\text{Sn}_\text{B}{}^t\text{Bu}_2\text{Li}$, **2** [50%]: $\delta = 132.5$; -42.8 ($^1J(^{119}\text{Sn-}^{119/117}\text{Sn}) = 6930/6610$ Hz); not classified signals: [5%] $\delta = -22.9$.

d) With KN(SiMe$_3$)$_2$ at -50 °C

$x = 2$ h; – ^{119}Sn{^{1}H} NMR (111.92 MHz, D_2O-capillary): $^t\text{Bu}_2\text{Sn}_\text{A}(\text{H})\text{Sn}_\text{B}{}^t\text{Bu}_2\text{K}$ [$> 90\%$]: $\delta = 126.8$ ($^1J(^{119}\text{Sn-}^{119/117}\text{Sn}) = 7700/7360$ Hz), $\delta = -43.5$ ($^1J(^{119}\text{Sn-}^1\text{H}) = 808$ Hz, $^1J(^{119}\text{Sn-}^{119/117}\text{Sn}) = 7700/7360$ Hz); not classified signals: [5%] $\delta = -22,2$; [$< 5\%$] $\delta = -35.0$.

Similar results are observed for using the sodium instead of the potassium amide.

e) With KH at −50 °C (10 fold excess KH)

$x = 4$ h; - ^{119}Sn{^{1}H} NMR (111.92 MHz, D_2O-capillary): $^t\text{Bu}_2\text{Sn}_\text{A}(\text{H})\text{Sn}_\text{B}{}^t\text{Bu}_2\text{K}$ [80%]: $\delta = 127.1$ ($^1J(^{119}\text{Sn-}^{119/117}\text{Sn}) = 7700/7360$ Hz), $\delta = -43.3$ ($^1J(^{119}\text{Sn-}^1\text{H}) = 808$ Hz, $^1J(^{119}\text{Sn-}^{119/117}\text{Sn}) = 7700/7355$ Hz); $^t\text{Bu}_2\text{Sn(K)Sn}{}^t\text{Bu}_2\text{K}$ [15%]: $\delta = 16.8$; not classified signals: [5%] $\delta = -23.2$.

Example for reactions with $^n\text{Alkyl}_2\text{SnH}_2$

1 g (4.25 mmol) $^n\text{Bu}_2\text{SnH}_2$; 5 ml (8.5 mmol) of a 1.7 M ^{t}BuLi/^{n}hexane solution; reaction temperature: −50 °C, reaction time 2 h. The solution was separated from the resulting solid by filtration (G3).

Colourless solid: The solid reacted slowly with water (bubbling) and the resulting solution was investigated by titration with HCl. The result strongly indicates that the colourless precipitate was pure LiH.

Solution: ^{119}Sn{^{1}H} NMR (111.92 MHz, D_2O-capillary): [45%] $\delta = 12.8$, [5%] $\delta = 3.4$, [25%] $\delta = -1.3$, [25%] $\delta = -5.7$.

GC-MS: Column CP-SIL-5CB (25 m), solvent: diethyl ether, 40 ml/min), 4 signals with retention times of 5.85; 7.12; 7.75 and 8.35 min. with a ratio of 2:15:70:13.

5.85 min. [2%]: no successful mass spectra could be obtained.

7.12 min. [15%]: *m/z*: 291 [80%], 235 [80%], 172 [BuSn, 100%].

7.75 min. [70%]: *m/z*: 374 [$^t\text{Bu}_2\text{BuSnCH}_2\text{CH}_2(^t\text{Bu})$, 100%],

317 [M^+-$\text{CH}_2\text{CH}_2{}^t\text{Bu}$, 40%], 175 [^{t}BuSn, 100%].

8.35 min. [13%]: *m/z*: 346 [$\text{Bu}_2\text{Sn}(^t\text{Bu})_2$, 100%], 235 [80%], 316 [M^+ -2 CH_3, 40%].

*General procedure for the formation of compounds (**4** – **9**)*

To a solution of 0.5 mmol of a bis(triorganylsilyl)diorganostannane and 140 mg (0.530 mmol) 18crown6 in 2 ml DME or thf, 21 mg (0.523 mmol) KH are added with stirring. Upon addition the reaction immediately turns yellow to red under slight gas evolution. An aliquot of the reaction mixture was used for NMR spectroscopy. For ^{29}Si and ^{119}Sn NMR shifts see Table 5.

Dimethyl(trimethylsilyl)stannyl potassium (**4**)

Starting materials: 150 mg (0.508 mmol) dimethylbis(trimethylsilyl)stannane; 2 ml DME, 21 mg (0.512 mmol) KH, 140 mg (0.530 mmol) 18crown6.

Diphenyl(trimethylsilyl)stannyl potassium (**5**)

Starting materials: 150 mg (0.358 mmol) diphenylbis(trimethylsilyl)stannane; 2 ml DME, 15 mg (0.36 mmol) KH; 95 mg (0.36 mmol) 18crown6.

Dimethyl(dimethylphenylsilyl)stannyl potassium (**6**)

Starting materials: 201 mg (0.48 mmol) dimethylbis(dimethylphenylsilyl)stannane; 2 ml DME, 20 mg (0.49 mmol) KH, 132 mg (0.5 mmol) 18crown6.

Di^{t}butyl(methyldiphenylsilyl)stannyl potassium (**7**)

Starting materials: 2.57 g (4.1 mmol) di^{t}butylbis(methyldiphenylsilyl)stannane; 15 ml thf, 168 mg (4.2 mmol) KH, 1.12 g (4.2 mmol) 18crown6, reaction time 48 h.

Dimethyl(triphenylsilyl)stannyl potassium (**8**)

Starting materials: 427 mg (0.64 mmol) dimethylbis(triphenylsilyl)stannane; 15 ml DME, 26 mg (0.63 mmol) KH, 169 mg (0.64 mmol) 18crown6, reaction time 48 h.

Di^{t}butyl(triphenylsilyl)stannyl potassium (**9**)

Starting materials: 1.57 g (2.1 mmol) di^{t}butylbis(triphenylsilyl)stannane; 15 ml DME, 90 mg (2.2 mmol) KH, 0.528 mg (2.0 mmol) 18crown6, reaction time 48 h.

General procedure for the formation of the triphenylsilyl (diphenylmethylsilyl)di^t butylstannanes **10** *and* **11**

To a cooled solution (−30 °C) of 4.0 mmol potassium di^{t}butyl(triorganosilyl)stannide in 50 ml DME or thf was

added drop wise a solution of dimethylphenylchlorosilane (0.69 g, 4.1 mmol) in *n*-hexane. The reaction mixture was slowly warmed to room temperature, the solvents were evaporated and the resulting residues were examined by ^{119}Sn and ^{29}Si NMR spectroscopy.

Dimethylphenylsilyl(diphenylmethylsilyl) di^{t}butylstannane (**10**)

Solvent: thf; ^{29}Si{^{1}H} NMR (59.63 MHz, D_2O/n-hexane): $\delta = -11.4$ (*Si*PhMe$_2$, $^1J_{^{29}Si-^{119/117}Sn}$: 387/370 Hz), $\delta = -10.0$ (*Si*Ph$_2$Me, $^1J_{^{29}Si-^{119/117}Sn} = 379/362$ Hz); ^{119}Sn{^{1}H} NMR (111.92 MHz, D_2O/^{n}hexane) $\delta = -185.1$.

Triphenylsilyl(diphenylmethylsilyl) di^{t}butylstannane (**11**)

Solvent: DME; ^{29}Si{^{1}H} NMR (59.587 MHz, C_6D_6): $\delta = -12.0$ (*Si*PhMe$_2$, $^1J_{^{29}Si-^{119/117}Sn}$: 385/368 Hz), $\delta = -8.1$ (*Si*Ph$_2$Me, $^1J_{^{29}Si-^{119/117}Sn} = 393/376$ Hz); ^{119}Sn{^{1}H} NMR (111.817 MHz, C_6D_6) $\delta = -183.6$.

Isolation of **10**

The isolation of **10** was following the procedure described in literature [12]. The residue was dissolved in 50 ml of ^{n}hexane, and hydrolyzed by addition of 10 ml of water. The organic layer was separated and dried over calcium chloride. After filtration (G3) and evaporation of the solvents the resulting crude product was purified by column chromatography (silica gel 60, hexane) to give 1.36 g (35%) of **10** as a colorless solid, m.p. 67 – 68 °C. Elemental analysis for $C_{29}H_{42}Si_2Sn$ (565.52 g/mol): calcd. C 61.59, H 7.43; found C 61.8, H 7.5.

Crystallography of **3**

The crystal was mounted on the diffractometer in a sealed Lindemann capillary. The data were collected at −182 °C to a maximum θ of 27.48° with 360 frames *via* ω-rotation ($\Delta/\omega = 1°$) twice 10s per frame on a Nonius Kappa CCD diffractometer using graphite monochromated Mo-K$_\alpha$ radiation ($\alpha = 0.71073$ Å). The structure was solved by Direct Methods (SHELXS97) [26] missing atoms, including the hydrogen atom bound to Sn(1), were located in subsequent Difference Fourier cycles and refined by full-matrix least-squares of F^2 (SHELXL97) [27]. All other hydrogen atoms were placed geometrically and refined using a riding model with a common isotropic temperature factor (C-H$_{prim.}$ 0.96 Å, U_{iso} 0.147(10) Å^2). All non-hydrogen atoms were refined using anisotropic displacement parameters. Only Sn(1), O(1), O(2), Li(1), and C(22) are not disordered, the other atoms are disordered over two sites with an occupancy of 0.5.

Crystallography of **10**

The crystal was mounted on the diffractometer as described previously [28]. Intensity data were collected at −182 °C with graphite monochromated Mo-K$_\alpha$ radiation ($\alpha = 0.71073$ Å), using a Siemens SMART system, complete with 3-circle goniometer and CCD detector operating at −54 °C. Details regarding instrumentation and data treatment have been reported previously [29]. An absorption correction was applied utilizing the program SADABS [30]. The crystal structure was solved by Direct Methods, as included in the SHELXTL-Plus program package [31]. Missing atoms, including the hydrogen atoms on Si and Sn, were located in subsequent difference Fourier maps and included in the refinement. Remaining hydrogen atoms were placed geometrically and refined using a riding model with U_{iso} constrained at 1.2 for non-methyl groups and 1.5 for methyl groups times U_{eq} of the carrier C atom. The structure was refined by full-matrix least-squares refinement on F^2 (SHELX-93) [32]. Scattering factors were those provided with the SHELX program system. All non-hydrogen atoms, with the exception of some disordered or restrained positions were refined anisotropically. Disorder was handled by including split positions for the affected groups, and included in the refinement of the respective occupancies. A set of restraints was applied to aid in modeling the disorder.

Atomic scattering factors for neutral atoms and real and imaginary dispersion terms were taken from International Tables for X–ray Crystallography [33]. The figures were created by SHELXTL (Sheldrick 1997) [34]. Full details for the structural analysis have been deposited with the Cambridge Crystallographic Data Centre, CCDC No. 257226 for compound **3**, CCDC No. 257167 for compound **10**. Copies of data can be obtained free of charge on application to The Director, CCDC, 12 Union Road, Cambridge CB2 1EZ, UK (Fax: int.code +(1223)336-033; e-mail: teched@chemcrys.cam.ac.uk), and are also available in CIF format from the authors.

Acknowledgements

The authors thank funds from the Graz University of Technology (Austria), the Deutsche Forschungsgemeinschaft (DFG, Germany) and the Fonds der chemischen Industrie (Germany). KRS is grateful for support by Syracuse University, the National Science Foundation (CHE-9702246) and the W. M. Keck Foundation. We also acknowledge Prof. Dr. K. Hassler (Graz University of Technology) for his interest in this work and donating the bis(triphenylsilyl)diorganostannanes to our disposal.

[1] P. Riviere, A. Castel, M. Riviere-Baudet, Alkaline and alkaline earth metal-14 compounds: Preparation, spectroscopy and reactivity, in: Z. Rappoport (ed.): The chemistry of organo-germanium, tin, and lead compounds (Chemistry of functional groups), pp. 653, John Wiley & Sons, Chichester (2002).
[2] J. P. Quintard, M. Pereyre, Reviews on Silicon, Germanium, Tin and Lead Compounds **4 (3)**, 151 (1980).
[3] Y. Matsuhashi, N. Tokitoh, R. Okazaki, M. Goto, S. Nagase, Organometallics **12**, 1351 (1993).
[4] M.-F. Connil, B. Jousseaume, M. Pereyre, Organometallics **15**, 4469 (1996).
[5] S. P. Mallela, R. A. Geanangel, Inorg. Chem. **32**, 5623 (1993).
[6] T. Lobreyer, W. Sundermeyer, H. Oberhammer, Chem. Ber. **127**, 2111 (1994).
[7] F. Uhlig, C. Kayser, R. Klassen, U. Hermann, L. Brecker, M. Schürmann, K. Ruhlandt-Senge, U. Englich, Z. Naturforsch. **54b**, 278 (1999).
[8] P. Bleckmann, U. Englich, U. Hermann, I. Prass, K. Ruhlandt-Senge, M. Schürmann, C. Schwittek, F. Uhlig, Z. Naturforsch. **54b**, 1188 (1999).
[9] U. Englich, I. Prass, K. Ruhlandt-Senge, T. Schollmeier, F. Uhlig, Monatsh. Chem. **133**, 931 (2002).
[10] M. Schürmann, T. Schollmeier, F. Uhlig, unpublished results.
[11] U. Hermann, G. Reeske, M. Schürmann, F. Uhlig, Z. Anorg. Allg. Chem. **627**, 453 (2001).
[12] M. Schürmann, I. Prass, F. Uhlig, Organometallics **19**, 2546 (2000).
[13] U. Englich, U. Hermann, I. Prass, T. Schollmeier, K. Ruhlandt Senge, F. Uhlig, J. Organomet. Chem. **646**, 271 (2001).
[14] G. Wittig, F. J. Meier, G. Lange, Liebigs Ann. Chem. **571**, 167 (1951).
[15] W. C. Still, J. Am. Chem. Soc. **100**, 1481 (1978).
[16] R. J. P. Corriu, C. Guerin, J. Organomet. Chem. **197**, C19 (1980).
[17] S. Sharma, A. C. Oelschlaeger, J. Org. Chem. **54**, 5064 (1989).
[18] D. Reed, D. Stalke, D. S. Wright, Angew. Chem. **103**, 1539 (1991).
[19] W. Reimann, H. G. Kuivila, D. Farah, T. Apoussidis, Organometallics **6**, 557 (1987).
[20] D. Farah, T. J. Carol, H. G. Kuivila, Organometallics, **4**, 662 (1985).
[21] D. Reed, D. Stalke, D. S. Wright, Angew. Chem. **103**, 1539 (1991).
[22] P. B. Hitchcock, M. F. Lappert, G. A. Lawless, B. Royo, J. Chem. Soc., Chem. Commun. 554 (1993).
[23] U. Englich, K. Ruhlandt-Senge, F. Uhlig, J. Organomet. Chem. **613**, 139 (2000).
[24] R. Fischer, J. Baumgartner, C. Marschner, F. Uhlig, in preparation.
[25] K. Hassler, unpublished results.
[26] G. M. Sheldrick, Acta Crystallogr. **A46**, 467 (1990).
[27] G. M. Sheldrick, SHELXL-97, University of Göttingen, Germany (1997).
[28] S. Chadwick, U. Englich, B. Noll, K. Ruhlandt-Senge, Inorg. Chem. **37**, 4718 (1998).
[29] H. Hope, Progr. Inorg. Chem. **41**, 1 (1994).
[30] G. M. Sheldrick, SADABS, Program for Absorption Correction Using Area Detector Data; University of Göttingen, Germany (1996).
[31] Siemens SHELXTL-Plus, Siemens: Madison, Wisconsin (1996).
[32] G. M. Sheldrick, SHELXL-93, University of Göttingen, Germany (1993).
[33] International Tables for Crystallography, Vol. C, Kluwer Academic Publishers, Dordrecht (1992).
[34] G. M. Sheldrick, SHELXTL, Release 5.1 Software Reference Manual, Bruker AXS Inc., Madison, Wisconsin (1997).